

Distributed Self-Concatenated Codes for Low-Complexity Power-Efficient Cooperative Communication

Muhammad Fasih Uddin Butt^{1,2}, Raja Ali Riaz^{1,2}, Soon Xin Ng¹ and Lajos Hanzo¹

¹School of ECS, University of Southampton, SO17 1BJ, United Kingdom.

Email: {mfub06r, rar06r, sxn, lh}@ecs.soton.ac.uk, <http://www-mobile.ecs.soton.ac.uk>

²Dept of EE, COMSATS Institute of Information Technology, Islamabad, 44000, Pakistan, <http://ciit.edu.pk>

Abstract—In this contribution, we propose a Distributed Binary Self-Concatenated Coding scheme using Iterative Decoding (DSECCC-ID) for cooperative communications. The DSECCC-ID scheme is designed with the aid of binary Extrinsic Information Transfer (EXIT) charts. The source node transmits SECCC symbols to both the relay and the destination nodes during the first transmission period. The relay performs SECCC-ID decoding. It then re-encodes the information bits using a Recursive Systematic Convolutional (RSC) code during the second transmission period. The resultant symbols transmitted from the source and relay nodes can be viewed as the coded symbols of a three-component parallel-concatenated SECCC-ID encoder. At the destination node, three-component DSECCC-ID decoding is performed. It is shown that the performance of the DSECCC-ID exactly matches the EXIT chart analysis. The EXIT chart gives us an insight into operation of the distributed coding scheme which enables us to significantly reduce the transmit power of the system.

I. INTRODUCTION

Digital communication exploiting multiple-input multiple-output (MIMO) wireless channels has recently attracted considerable attention. The wireless communication systems of future generations are required to provide reliable transmissions at high data rates in order to offer a variety of multimedia services to commercial wireless products and networks. Space time coding schemes [1], which employ multiple transmitters and receivers, are among the most efficient techniques designed for achieving a high diversity gain, provided that the associated Multiple-Input Multiple-Output (MIMO) channels [2], [3] experience independent fading. Utilising cooperative techniques eliminates the correlation of the signals when using multiple antennas at the mobiles which is imposed by the limited affordable element-spacing. Cooperative diversity schemes were proposed in [4]–[6], whereby, each mobile unit collaborates with one partner or a few partners for the sake of reliably transmitting both its own information and that of its partners jointly, which emulates a virtual MIMO scheme. The two most popular collaborative protocols used between the source, relay and destination nodes are the Decode-And-Forward (DAF) as well as the Amplify-And-Forward (AAF) schemes. However, a strong channel code is required for mitigating the potential error propagation in the DAF scheme or for mitigating the noise enhancement at the destination of the AAF-aided scheme.

The philosophy of concatenated coding schemes was proposed by Forney in [7]. Turbo codes, which were developed in [8] constitute a class of error correction codes (ECC) based on two or more parallel concatenated convolutional codes (PCCC) used as constituent codes. They are high-performance codes capable of operating near the Shannon limit. Since their invention they have found diverse applications in bandwidth-limited communication systems, where the maximum achievable information rate has to be supported in the presence of transmission errors due to both the ubiquitous Additive White Gaussian Noise (AWGN) and channel fading. Various bandwidth

The financial support of COMSATS Institute of Information Technology, Islamabad under the auspices of Higher Education Commission, Pakistan and that of the EPSRC UK, as well as of the EU Optimix project of the European Union is gratefully acknowledged.

efficient turbo codes were proposed in [9], [10] and [11]. Serially concatenated convolutional codes (SCCC) [12] have been shown to yield a performance comparable, and in some cases superior, to turbo codes. Iteratively-Decoded Self-Concatenated Convolutional Codes (SECCC-ID) proposed by Benedetto *et al.* [13] constitute another attractive family of iterative detection aided schemes. The SECCC arrangement is a low-complexity scheme using a single encoder and a single decoder. The Extrinsic Information Transfer (EXIT) chart based analysis of the iterative decoder provides an insight into its decoding convergence behaviour and hence it is helpful for finding the best constituent coding schemes for creating SECCCs.

The concept of EXIT charts was proposed in [14] as a tool designed for analysing the convergence behaviour of iteratively decoded systems. EXIT charts constitute a semi-analytical tool used to predict the SNR value, where an infinitesimally low Bit Error Ratio (BER) can be achieved without performing time-consuming bit-by-bit decoding employing a high number of decoding iterations.

Recently, various SECCC-ID schemes were designed in [15], [16] with the aid of EXIT charts for approaching the capacity of the Rayleigh fading channel. An SECCC-ID scheme was designed using Trellis Coded Modulation (TCM) as constituent codes with the aid of EXIT charts in [15]. The scheme proposed in [16] employs binary Recursive Systematic Convolutional (RSC) codes as constituent codes to eliminate the mismatch between the EXIT-curves and the Monte-Carlo simulation-based stair-case-shaped decoding trajectory inherited by the symbol-based TCM design by proposing a bit-based SECCC-ID design in order to create flexible SECCC schemes.

In this contribution, we propose a power and bandwidth efficient Distributed Self-Concatenated Coding scheme using iterative decoding (DSECCC-ID) for cooperative communications. Distributed turbo codes [17] have also been proposed for cooperative communications, although under the simplifying assumption of having a perfect communication link between the source and the relay nodes. Our design takes into consideration the realistic condition of having an imperfect source-relay communication link.

We first design a SECCC-ID scheme for the sake of achieving decoding convergence at low SNR, using EXIT charts. Then we invoke this SECCC-ID scheme for cooperative communications, where the source employs an SECCC-ID encoder and the relay employs both a hypothetical two-component SECCC-ID decoder as well as a single RSC encoder. At the destination, a novel three-component DSECCC-ID decoder is used. The decoding convergence of the three-component DSECCC-ID decoder to an infinitesimally low BER depends on the specific choice of the component codes as well as on the distance between the cooperating nodes.

The paper is organised as follows. The system model is described in Section II. The DSECCC-ID encoder and decoder are highlighted in Sections III and IV, respectively. The design and analysis of the proposed scheme is provided in Section V. Our simulation results are discussed in Section VI. Finally, our conclusions are offered in Section VII.

II. SYSTEM MODEL

The schematic of a two-hop relay-aided system is shown in Fig. 1, where the source node (*s*) transmits a frame of coded symbols \mathbf{x}_s to the relay node (*r*) and the destination node (*d*) during the first transmission period T_1 , while the relay node first decodes the information, then re-encodes it and finally transmits a frame of coded symbols \mathbf{x}_r to the destination node during the second transmission period T_2 . The communication links seen in Fig. 1 are subject to both free-space path loss as well as to short-term uncorrelated Rayleigh fading.

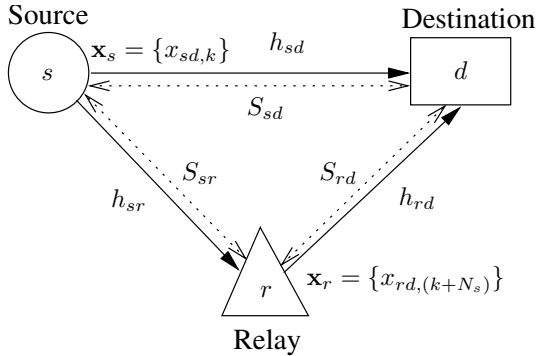


Fig. 1. Schematic of a two-hop relay-aided system, where S_{ab} is the geometrical distance between node *a* and node *b*.

Let S_{ab} denote the geometrical distance between nodes *a* and *b*. The path loss between these nodes can be modelled by [18]:

$$P(ab) = K/S_{ab}^\alpha, \quad (1)$$

where K is a constant that depends on the environment and α is the path loss exponent. For a free-space path loss model we have $\alpha = 2$. The relationship between the energy E_{sr} received at the relay node and that of the destination node E_{sd} can be expressed as:

$$E_{sr} = \frac{P(sr)}{P(sd)} E_{sd} = G_{sr} E_{sd}, \quad (2)$$

where G_{sr} is the power-gain (or geometrical gain) [18] experienced by the source-relay link with respect to the source-destination link as a benefit of its reduced distance and path loss, which can be computed as:

$$G_{sr} = \left(\frac{S_{sd}}{S_{sr}} \right)^2. \quad (3)$$

Similarly, the power-gain for the relay-destination link with respect to the source-destination link can be formulated as:

$$G_{rd} = \left(\frac{S_{sd}}{S_{rd}} \right)^2. \quad (4)$$

Naturally, the power-gain of the source-destination link with respect to itself is unity, i.e. $G_{sd} = 1$.

The k th received signal at the relay node during the first transmission period T_1 , where N_s number of symbols are transmitted from the source node, can be written as:

$$y_{sr,k}^{(T_1)} = \sqrt{G_{sr}} h_{sr,k}^{(T_1)} x_{sr,k}^{(T_1)} + n_{sr,k}^{(T_1)}, \quad (5)$$

where $k \in \{1, \dots, N_s\}$ and h_{sr} is the Rayleigh fading channel coefficient between the source node and the relay node at instant k , while n_{sr} is the zero mean complex AWGN having a variance of $N_0/2$ per dimension. By contrast, the k th received symbol at the destination node can be expressed as:

$$y_{sd,k}^{(T_1)} = h_{sd,k}^{(T_1)} x_{sd,k}^{(T_1)} + n_{sd,k}^{(T_1)}, \quad (6)$$

where h_{sd} is the Rayleigh fading channel coefficient between the source node and the destination node at instant k , while n_{sd} is

the AWGN having a variance of $N_0/2$ per dimension. Similarly, the l th received symbol at the destination node during the second transmission period T_2 , where N_r number of symbols are transmitted from the relay node, is given by:

$$y_{rd,l}^{(T_2)} = \sqrt{G_{rd}} h_{rd,l}^{(T_2)} x_{rd,l}^{(T_2)} + n_{rd,l}^{(T_2)}, \quad (7)$$

where $l \in \{1 + N_s, \dots, N_r + N_s\}$ and h_{rd} is the Rayleigh fading channel coefficient between the relay node and the destination node at instant l , while n_{rd} is the AWGN having a variance of $N_0/2$ per dimension.

III. DSECCC-ID ENCODER

In our DSECCC-ID scheme, we consider a Quadrature Phase-Shift Keying (QPSK)-assisted two-component SECCC encoder at the source node as well as a QPSK-assisted RSC encoder at the relay node. Note that the relay transmits only the parity bits during

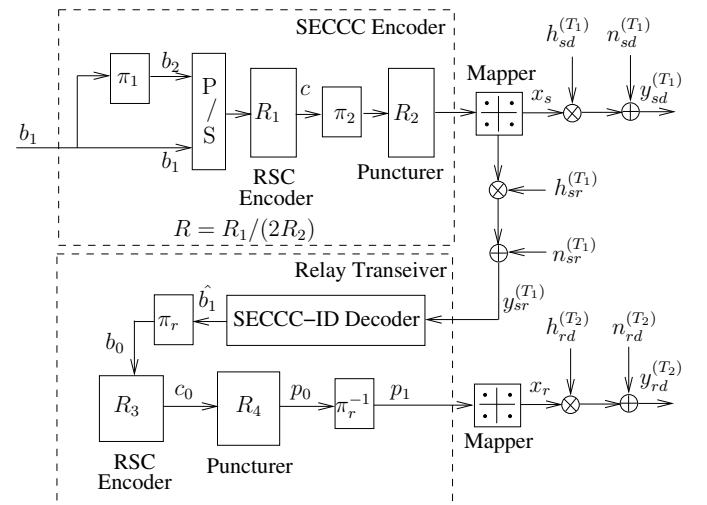


Fig. 2. The schematic of a three-component self-concatenated encoder. This figure applies to the DSECCC-ID scheme, when the relay transceiver node decodes the received symbols using SECCC-ID decoder and then forwards the decoded symbols to the destination in the second phase.

the first transmission period to ensure that the systematic bits are transmitted only once to the destination. The relay detects the signals received from the source node during the first transmission period. The notation π_r in Fig. 2 denotes the random bit interleaver used at the relay to interleave the decoded bits before the RSC encoding. The encoders employed at both the source and relay transceiver nodes can be viewed as a three-component parallel-concatenated SECCC-ID encoder, which is depicted in Fig. 2.

The notation x_r used in Fig. 2 denotes the 2-bit QPSK symbol at the relay node. The puncturer denoted as R_4 in Fig. 2 is used to improve the overall throughput of the scheme. We found that a good performance can be achieved by transmitting only the parity bits generated at the output of the RSC encoder at the relay node.

At the source node we consider a rate $R = 1/3$ SECCC scheme employing QPSK modulation. Uncorrelated Rayleigh fading channel conditions are considered for this analysis.

As shown in Fig. 2, the input bit sequence $\{b_1\}$ of the self-concatenated encoder is interleaved for yielding the bit sequence $\{b_2\}$. The resultant bit sequences are parallel-to-serial converted and then fed to the RSC encoder, which employs the generator polynomial $G=[13\ 15]$ expressed in octal format and having a rate of $R_1 = \frac{1}{2}$ and memory of $\nu = 3$. Hence, for every bit input to the SECCC encoder there are four output bits of the RSC encoder. At the output of the encoder there is an interleaver and then a rate $R_2 = \frac{3}{4}$ puncturer,

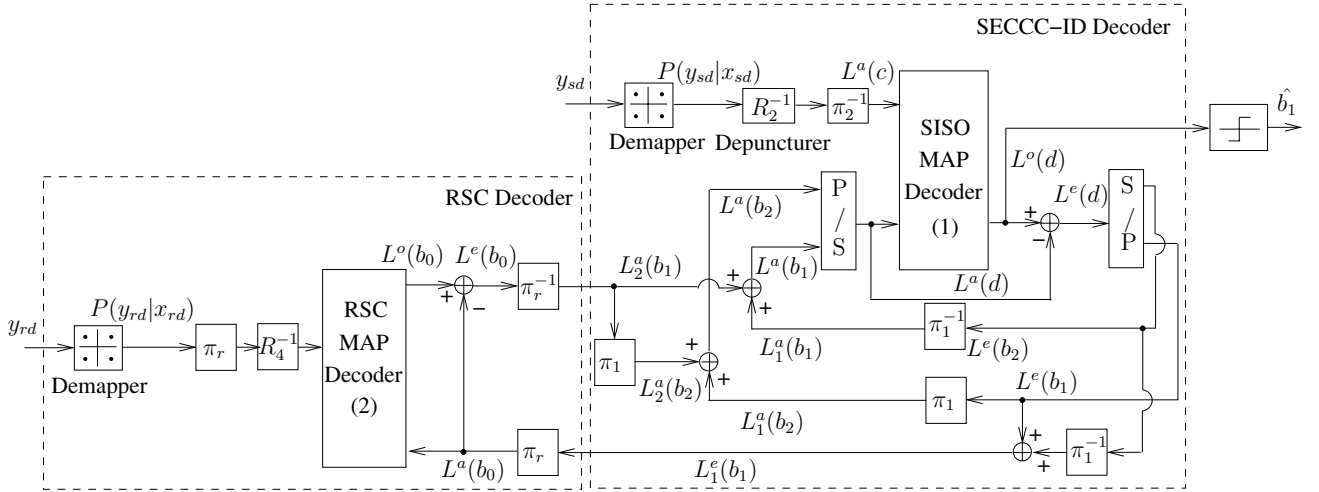


Fig. 3. The schematic of the DSECCC-ID decoder. The input to the SECCC-ID decoder is through the QPSK demapper for a source-destination link, while the input to the RSC decoder is through the QPSK demapper for a relay-destination link.

which punctures (does not transmit) one bit out of four encoded bits. Hence, the overall code rate, R can be derived based on [19] as:

$$R = \frac{R_1}{2 \times R_2} = \frac{1/2}{2(3/4)} = \frac{1}{3} \quad (8)$$

Puncturing is used in order to increase the achievable bandwidth efficiency η . Different codes have been designed in [16] by changing the rates R_1 and R_2 . These bits are then mapped to a QPSK symbol as $x = \mu(c_1 c_0)$, where $\mu(\cdot)$ is the bit-to-symbol mapping function. Hence the bandwidth efficiency is given by $\eta = R \times \log_2(4) = 0.67$ bit/s/Hz, assuming a Nyquist roll-off-factor of $\alpha=0$. The QPSK symbol x_s is then transmitted over the channel.

The overall throughput of this two-hop cooperative scheme can be formulated as:

$$\eta = \frac{N_i}{N_s + N_r} [\text{bps}], \quad (9)$$

where N_i is the number of information bits transmitted within a duration of $(N_s + N_r)$ symbol periods. Again, N_s is the number of modulated symbols per frame transmitted from the source node and N_r is the number of modulated symbols per frame arriving from the relay node. For our case we have $N_i = 120,000$ bits. Therefore, we transmit $N_s = 180,000$ symbols. Note that the number of symbols per transmission burst at the relay node is given by $N_r = 60,000$ due to the employment of QPSK modulation and a puncturer that removes all systematic bits from the RSC's output. Hence, the overall effective throughput of the DSECCC-ID scheme is given by $\eta = (N_i)/(N_s + N_r) = 0.5$ bps. The Signal to Noise Ratio (SNR) per bit is given by $E_b/N_0 = \text{SNR}/\eta$. Hence, the DSECCC-ID scheme suffers from a penalty of 1.25 dB in terms of E_b/N_0 , when compared to the conventional SECCC-ID scheme having a somewhat higher throughput of 0.67 bit/s/Hz.

IV. DSECCC-ID DECODER

The novel decoder structure of the DSECCC-ID scheme is illustrated in Fig. 3. The notations $P(\cdot)$ and $L(\cdot)$ in Fig. 3 denote the logarithmic-domain symbol probabilities and the Logarithmic-Likelihood Ratio (LLR) of the bit probabilities, respectively. The notations b and c in the round brackets (\cdot) in Fig. 3 denote information bits and coded bits, respectively. The specific nature of the probabilities and LLRs is represented by the subscripts a , o and e , which denote in Fig. 3, *a priori*, *a posteriori* and *extrinsic* information, respectively.

For the SECCC-ID decoder, denoted by (1) in Fig. 3, the received signal arrives at the soft demapper. This signal is then used by the

demapper for calculating the conditional probability density function (PDF) of receiving y , when x_s was transmitted, yielding:

$$P(y|x = x_s) = \frac{1}{\pi N_0} \exp\left(-\frac{|y - hx_s|^2}{N_0}\right), \quad (10)$$

where $x_s = \mu(c_1 c_0)$ is the hypothetically transmitted QPSK symbol for $s \in \{0, 1, 2, 3\}$, h is the channel's non-dispersive fading coefficient and n is the AWGN having a variance of $N_0/2$ per dimension. The extrinsic bit probabilities are then passed through a soft depuncturer, which converts them to the corresponding bit-based LLRs and subsequently inserts zero LLRs at the punctured bit positions. The LLRs are then deinterleaved and fed to the Soft-Input Soft-Output (SISO) *Maximum A Posteriori Probability* (MAP) decoder [20]. The decoder of Fig. 3 is a self-concatenated decoder. It first calculates the extrinsic LLRs of the information bits, namely $L^e(b_1)$ and $L^e(b_2)$. Then they are appropriately interleaved to yield the *a priori* LLRs of the information bits, namely $L^a(b_1)$ and $L^a(b_2)$, as shown in Fig. 3. Self-concatenated decoding proceeds, until a fixed number of iterations is reached.

There are two inputs to the RSC MAP decoder block, which is denoted by (2) in Fig. 3. The first is the extrinsic information of bit b_1 provided by the SECCC-ID decoder, which is denoted by (1). As seen in Fig. 3 this is obtained from the addition of $L^e(b_1)$ and the deinterleaved version of $L^e(b_2)$. The resultant $L_1^e(b_1)$ stream is interleaved by π_r to generate $L^a(b_0)$. The second input of the RSC MAP decoder (2) is the interleaved and depunctured version of the soft information provided by the QPSK demapper denoted as $P(y_{rd}|x_{rd})$ in Fig. 3. The RSC decoder of Fig. 3 at the relay node then provides the improved extrinsic LLR of the data bit b_0 namely $L^e(b_0)$ as its output, which is deinterleaved by π_r^{-1} to yield $L_2^a(b_1)$. The LLR $L_2^a(b_1)$ can be further interleaved using π_1 to generate $L_2^o(b_1)$. These *a priori* LLRs output by the RSC can be added to the SECCC-ID decoder's *a priori* LLRs of b_1 and b_2 , thus completing the iteration between the RSC and SECCC-ID decoders.

V. DESIGN AND ANALYSIS

Our code design procedure commences by calculating the decoding convergence of the SECCC-ID scheme at the output of the communication link between the source and the relay nodes, using EXIT charts.

Binary EXIT charts are useful for finding the best SECCC-ID schemes for having a decoding convergence at the lowest possible SNR value. The EXIT curves of the SECCC decoder components and a corresponding decoding trajectory were recorded for the best-performing binary SECCC schemes operating closest to the Rayleigh

channel's capacity, which are given in Fig. 4. These were recorded by using 10 transmission frames, each consisting of 24×10^3 information bits for calculating the EXIT curve, while we consider a frame size of 120×10^3 information bits for calculating the decoding trajectories¹.

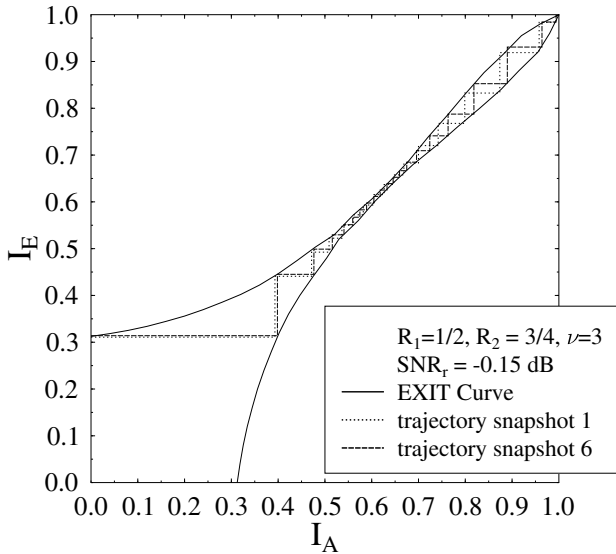


Fig. 4. EXIT chart and two 'snap-shot' decoding trajectories for $R_1=1/2$ and $R_2=3/4$, QPSK-assisted SECCC-ID, $\nu = 3$, $\eta = 0.67$ bit/s/Hz at $\text{SNR}_r = -0.15$ dB for transmission over an uncorrelated Rayleigh channel.

In Fig. 4, the scheme using $R_1 = 1/2$, $R_2 = 3/4$, $\nu = 3$ is analysed. As we can see from Fig. 4, a receive SNR of about -0.15 dB is needed in order to attain a decoding convergence to the (1,1) point of the EXIT chart, since at a receive SNR of -0.2 dB the EXIT-tunnel remains closed. Fig. 4 also corresponds to the performance of the SECCC-ID scheme of the source-relay link. The receive SNR can be computed as:

$$\text{SNR}_r = \text{SNR}_e + 10 \log_{10}(G_{sr}) \text{ [dB]}, \quad (11)$$

When there is no path-loss, the receive SNR equals the equivalent SNR^2 , denoted by SNR_e and G_{sr} was defined in (3). Hence, a receive SNR of -0.15 dB can be achieved by various combinations of SNR_e and G_{sr} . For this scheme the decoding convergence threshold³ is at -0.2 dB, when employing $I = 40$ self-concatenated iterations, which is 0.56 dB away from the Rayleigh channel's capacity [21]. This scheme acquires an open EXIT tunnel⁴ at $\text{SNR}_r = -0.15$ dB, when communicating over an uncorrelated Rayleigh fading channel.

In our analysis the relay node of the DSECCC-ID is assumed to be placed half-way between the source and relay nodes, i.e. we have $G_{sr} = G_{rd} = 4$, hence the minimum required equivalent SNR at the source node is $\text{SNR}_e = -0.15 - 6.02 = -6.17$ dB.

In this section the decoding convergence of the three-component DSECCC-ID decoder at the destination node is then analysed. The EXIT curves of the SECCC-ID decoder at the source-destination link

¹we need large interleaver sizes for the trajectories to match the EXIT curves, whereas for the EXIT curves less bits can give us good prediction [14].

²To simply our analysis the term of equivalent SNR is introduced, which is the ratio of the signal power at the transmitter (source/relay node) with respect to the noise level at the receiver (relay/destination node).

³the SNR value beyond which the EXIT tunnel becomes 'just' open, although this does not necessarily imply that the $(I_A, I_E)=(1,1)$ point of 'perfect convergence' can be reached because some of the decoding trajectories are curtailed owing to the limited interleaver length used.

⁴specifies the equivalent SNR value where there is a more widely open EXIT tunnel leading to the (1,1) point and where decoding convergence to an infinitesimally low BER value can always be achieved, provided that the interleaver length is beyond a certain value and the number of iterations is sufficiently high [14].

employing $I_{sd} = 2$ self iterations as well as that of the RSC decoder at the relay-destination link are plotted in Fig. 5. Both the SECCC-ID and the RSC employ same complexity MAP decoder.

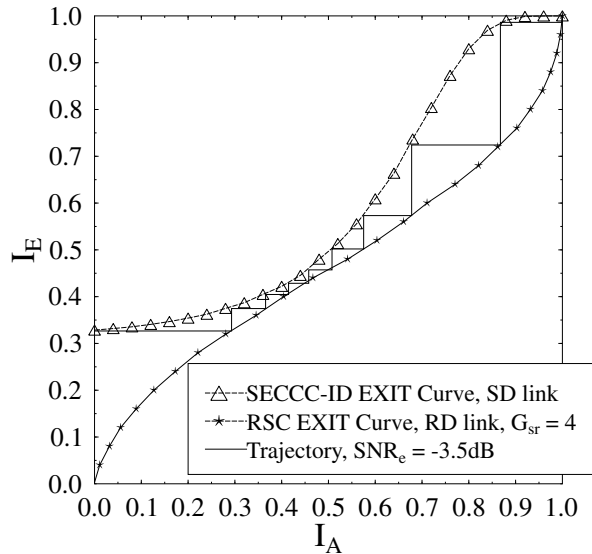


Fig. 5. The EXIT curves and a decoding trajectory of the DSECCC-ID scheme for a $\text{SNR}_e = -3.5$ dB both at the source as well as at the relay nodes.

The threshold for the DSECCC-ID system can be calculated from the EXIT curves intersecting each other at SNR_e of -3.65 dB. Hence the trajectory will not reach the (1,1) point of perfect convergence to a vanishingly low BER. But once the system is working at $\text{SNR}_e = -3.5$ dB at the source-destination link and again at $\text{SNR}_e = -3.5$ dB at the relay-destination link, we get an open tunnel. Since $\text{SNR}_e = -3.5$ dB is higher than the threshold of $\text{SNR}_e = -6.17$ dB, which guarantees a SECCC-ID decoding convergence at the relay, we can safely assume a near-perfect source-to-relay link. Another reason why we are operating at a higher SNR is because we want to have less self-concatenated iterations at the source-relay link, namely $I_{sr} = 8$ in this case. The number of iterations between the SECCC-ID and RSC at the destination node is limited to $I_{sd,rd} = 12$. Therefore, at the DSECCC-ID decoder we have $I_{DSCC} = I_{sd} \times I_{sd,rd} = 24$ decoding iterations. This makes the total decoding iterations in the overall system equal to $I_{sr} + I_{DSCC} = 32$ as compared to a non-cooperative SECCC-ID employing $I = 40$ iterations. The EXIT chart analysis thus helps us analyse this cooperative communications system and this insight allows us to reduce the equivalent SNR at the source and the relay as well as the complexity at the relay and the destination.

The EXIT chart analysis is verified by computing the corresponding Monte-Carlo simulation based decoding trajectory for the DSECCC-ID scheme. The distinct decoding trajectory based on a frame length of 120 000 bits is shown in Fig. 5 for an equivalent SNR of -3.5 dB both at the source and at the relay. It matches the EXIT curves generated for the source-destination link, which employs the SECCC-ID scheme and the relay-destination link which employs RSC scheme, hence, verifying the predicted results.

VI. RESULTS AND DISCUSSIONS

Finally, we compare the achievable performance of the DSECCC-ID scheme employing a realistic relay node, which potentially induces error propagation, to that of the non-cooperative SECCC-ID scheme. The Bit Error Ratio (BER) versus equivalent SNR performance of the DSECCC-ID and SECCC-ID schemes is shown in Fig. 6.

The SECCC-ID scheme has a decoding threshold at -0.2 dB and the tunnel at -0.15 dB. The DSECCC-ID system has been analysed

at -3.5 dB at the source and the relay employing the RSC encoder. Thus the DSECCC-ID outperforms the SECCC-ID scheme by about 3.35 dB in SNR terms, which corresponds to $3.35 - 1.25 = 2.1$ dB in terms of E_b/N_0 .

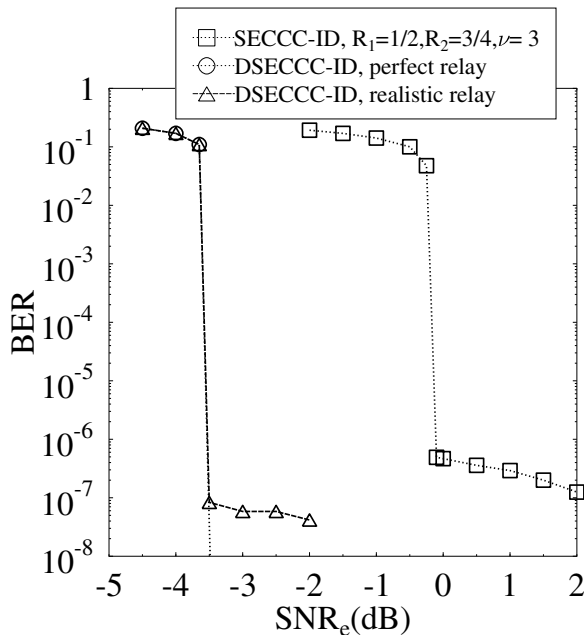


Fig. 6. BER versus equivalent SNR performance of the DSECCC-ID and SECCC-ID schemes for a frame length of 120,000 bits.

The performance of the DSECCC-ID scheme in conjunction with perfect relaying is seen in Fig. 6, which matches the EXIT chart based prediction, as illustrated in Fig. 5. Furthermore, the BER performance of the DSECCC-ID scheme using perfect relaying matches the performance of the DSECCC-ID scheme involving realistic error-prone relaying except for the fact that it does not have an error floor region, as shown in Fig. 6. The DSECCC-ID scheme assuming a realistic relay has an error floor due to that of the SECCC-ID decoder employed at the relay. The tunnel as predicted by the EXIT charts seen in Fig. 5 is at -3.5 dB, where all the trajectories reach the (1,1) point. The corresponding BER curve shown in Fig. 6 matches this prediction. This makes DSECCC-ID an attractive low-power relaying scheme.

VII. CONCLUSION

A power and bandwidth efficient DSECCC-ID scheme has been proposed for cooperative communications based on the three-component design of Fig. 3. The best-performing SECCC-ID scheme is required at the relay node in order to minimise the decoding error probability at the minimum possible equivalent SNR. Once the received SNR at the relay node exceeds the error-free decoding threshold, the SECCC-ID decoder employed at the relay node becomes capable of reliably decoding the source signals. The relay node employs a simple RSC encoder and only its parity bits are transmitted to the destination node. The EXIT chart of the three-component DSECCC-ID decoder seen in Fig. 5 reveals that a beneficial combination of the equivalent SNR of the source and the relay nodes results in a low BER at the destination despite considering a potentially error-prone reception at the relay. Thus we reduced the total power required by the overall system as compared to an SECCC-ID system. Also the overall complexity of this distributed cooperative communication system is less than a non-cooperative SECCC-ID system. Our simulation results seen in Fig. 6 show that the DSECCC-ID, employing a low-complexity SECCC-ID scheme is a power-efficient scheme in the scenario of a relay placed about half-way between the source and destination nodes. Our future research

will focus on enhancing this DSECCC-ID scheme designed for cooperative communications to operate near the capacity without excessive complexity and will study its performance for different relay location scenarios and power allocations. Furthermore, we will investigate the performance of such DSECCC-ID schemes in differentially encoded, non-coherently detected cooperative systems.

REFERENCES

- [1] V. Tarokh, N. Seshadri, and A. R. Calderbank, "Space-time codes for high data rate wireless communication: Performance criterion and code construction," *IEEE Transactions on Information Theory*, vol. 44, pp. 744–765, March 1998.
- [2] G. Foschini Jr. and M. Gans, "On limits of wireless communication in a fading environment when using multiple antennas," *Wireless Personal Communications*, vol. 6, pp. 311–335, March 1998.
- [3] S. X. Ng and Hanzo, "On the MIMO Channel Capacity of Multi-Dimensional Signal Sets," *IEEE Transactions on Vehicular Technology*, vol. 55, pp. 528–536, March 2006.
- [4] A. Sendonaris, E. Erkip and B. Aazhang, "User cooperation diversity part I: System description," *IEEE Transactions on Communications*, vol. 51(11), pp. 1927–1938, 2003.
- [5] N. Laneman, D. N. C. Tse and G. W. Wornell, "Cooperative diversity in wireless networks: efficient protocols and outage behavior," *IEEE Trans. on Information Theory*, vol. 50, no. 12, pp. 3062–3080, 2004.
- [6] E. Zimmermann, P. Herhold and G. Fettweis, "On the performance of cooperative relaying protocols in wireless networks," *European Transactions on Telecommunications*, vol. 16, no. 1, pp. 5–16, 2005.
- [7] G. Forney, *Concatenated Codes*. MIT Press, 1966.
- [8] C. Berrou and A. Glavieux, "Near optimum error correcting coding and decoding: Turbo codes," *IEEE Transactions on Communications*, vol. 44, pp. 1261–1271, October 1996.
- [9] S. Le Goff, A. Glavieux, and C. Berrou, "Turbo-codes and high spectral efficiency modulation," in *IEEE International Conference on Communications*, (New Orleans, LA, USA), pp. 645–649, May 1994.
- [10] S. Benedetto, D. Divsalar, G. Montorsi, and F. Pollara, "Bandwidth efficient parallel concatenated coding schemes," *Electronics Letters*, vol. 31, pp. 2067–2069, Nov. 1995.
- [11] P. Robertson and T. Wörz, "Coded modulation scheme employing turbo codes," *IEE Electronics Letters*, vol. 31, pp. 1546–1547, 31st August 1995.
- [12] S. Benedetto, D. Divsalar, G. Montorsi, and F. Pollara, "Serial concatenated trellis coded modulation with iterative decoding," in *IEEE International Symposium on Information Theory*, (Ulm), p. 8, June/July 1997.
- [13] S. Benedetto, D. Divsalar, G. Montorsi, and F. Pollara, "Self-concatenated trellis coded modulation with self-iterative decoding," in *IEEE Global Telecommunications Conference*, vol. 1, (Sydney, NSW, Australia), pp. 585–591, 1998.
- [14] S. ten Brink, "Convergence behavior of iteratively decoded parallel concatenated codes," *IEEE Transactions on Communications*, vol. 49, pp. 1727–1737, Oct. 2001.
- [15] M. F. U. Butt, S. X. Ng, and L. Hanzo, "EXIT chart aided design of near-capacity self-concatenated trellis coded modulation using iterative decoding," in *67th IEEE Vehicular Technology Conference, VTC '08 Spring*, (Marina Bay, Singapore), pp. 734–738, May 2008.
- [16] M. F. U. Butt, R. A. Riaz, S. X. Ng, and L. Hanzo, "Near-capacity iteratively decoded binary self-concatenated code design using EXIT charts," in *IEEE Global Communications Conference, GLOBECOM '08*, (New Orleans, USA), Nov./Dec. 2008.
- [17] B. Zhao and M. C. Valenti, "Distributed turbo coded diversity for relay channel," *IEE Electronics Letters*, vol. 39, pp. 786–787, May 2003.
- [18] H. Ochiai, P. Mitran and V. Tarokh, "Design and analysis of collaborative diversity protocols for wireless sensor networks," in *Proceedings of IEEE VTC Fall*, (Los Angeles, USA), pp. 4645 – 4649, 26-29 September 2004.
- [19] J. Hagenauer, "Rate-compatible punctured convolutional codes (RCPC codes) and their applications," *IEEE Transactions on Communications*, vol. 36, pp. 389–400, Apr. 1988.
- [20] S. Benedetto, D. Divsalar, G. Montorsi, and F. Pollara, "A soft-input soft-output APP module for iterative decoding of concatenated codes," *IEEE Communication Letters*, pp. 22–24, 1997.
- [21] L. Hanzo, S. X. Ng, T. Keller, and W. Webb, *Quadrature amplitude modulation: From basics to adaptive trellis-coded, turbo-equalised and space-time coded OFDM, CDMA and MC-CDMA systems*, pp. 746–748. Wiley-IEEE Press, 2nd ed., December 15, 2004.